NeuroImage 59 (2012) 1571–1581

Contents lists available at SciVerse ScienceDirect

NeuroImage

journal homepage: www.elsevier.com/locate/ynimg

The primary somatosensory cortex largely contributes to the early part of the cortical response elicited by nociceptive stimuli

E. Valentini [a,b,1], L. Hu [c,d,1], B. Chakrabarti [e,f], Y. Hu [d], S.M. Aglioti [b], G.D. Iannetti [a,*]

[a] Department of Neuroscience, Physiology and Pharmacology, University College London, UK
[b] Fondazione Santa Lucia and Department of Psychology, "La Sapienza" University of Rome, Italy
[c] Key Laboratory of Cognition and Personality (Ministry of Education) and School of Psychology, Southwest University, Chongqing, China
[d] Department of Orthopaedics and Traumatology, The University of Hong Kong, Hong Kong, China
[e] Centre for Integrative Neuroscience and Neurodynamics, School of Psychology and Clinical Language Sciences, University of Reading, Reading, UK
[f] Autism Research Centre, Department of Psychiatry, University of Cambridge, Cambridge, UK

ARTICLE INFO

Article history:
Received 24 June 2011
Revised 18 August 2011
Accepted 21 August 2011
Available online 28 August 2011

Keywords:
Laser-evoked potentials (LEPs)
Nociception
Postcentral gyrus
Primary somatosensory cortex
Source analysis

ABSTRACT

Research on the cortical sources of nociceptive laser-evoked brain potentials (LEPs) began almost two decades ago (Tarkka and Treede, 1993). Whereas there is a large consensus on the sources of the late part of the LEP waveform (N2 and P2 waves), the relative contribution of the primary somatosensory cortex (S1) to the early part of the LEP waveform (N1 wave) is still debated.

To address this issue we recorded LEPs elicited by the stimulation of four limbs in a large population (n = 35). Early LEP generators were estimated both at single-subject and group level, using three different approaches: distributed source analysis, dipolar source modeling, and probabilistic independent component analysis (ICA). We show that the scalp distribution of the earliest LEP response to hand stimulation was maximal over the central-parietal electrodes *contralateral* to the stimulated side, while that of the earliest LEP response to foot stimulation was maximal over the central-parietal *midline* electrodes. Crucially, all three approaches indicated hand and foot S1 areas as generators of the earliest LEP response.

Altogether, these findings indicate that the earliest part of the scalp response elicited by a selective nociceptive stimulus is largely explained by activity in the contralateral S1, with negligible contribution from the secondary somatosensory cortex (S2).

Introduction

Brief laser heat pulses selectively excite Aδ- and C-fiber epidermal free nerve endings (Bromm and Treede, 1984). Such stimuli elicit a number of transient brain responses (laser-evoked potentials, LEPs) in the ongoing electroencephalogram (EEG) (Carmon et al., 1976; Mouraux et al., 2003). These responses are mediated by the activation of type-II Aδ mechano-heat nociceptors (II-AMH) (Treede, 1995) and spinothalamic neurons in the anterolateral quadrant of the spinal cord (Treede, 2003). LEPs consist of a number of deflections. The largest of these deflections form a negative–positive complex (N2–P2), peaking at approximately 200–350 ms when stimulating the hand dorsum and maximal at the scalp vertex (Bromm and Treede, 1984). This complex is preceded by a smaller negative deflection (N1) peaking at approximately 160 ms when stimulating the hand dorsum and maximal over the central-temporal region contralateral to the stimulated side (Tarkka and Treede, 1993). Although Aδ-related LEPs are widely used to investigate the peripheral and central processing of nociceptive sensory input (Iannetti et al., 2003; Treede et al., 2003), and are currently considered the best available diagnostic tool to assess the function of Aδ nociceptive pathways in patients (Haanpaa et al., 2011), a full understanding of their functional significance remains to be achieved.

A crucial step in this direction is a compelling description of the cortical sources underlying the earliest part of the LEP response. Indeed, while there is converging evidence from dipolar modeling of both scalp and subdural recordings, as well as from direct intracranial recordings, that the bilateral operculoinsular cortex and the cingulate cortex generate, albeit with different contributions, the late-latency N2 and P2 waves (Frot and Mauguiere, 2003; Frot et al., 2007, 2008; Kakigi et al., 1995; Kanda et al., 2000; Perchet et al., 2008; Tarkka and Treede, 1993; Valeriani et al., 1996, 2000; Vogel et al., 2003), the contribution of the controlateral primary somatosensory cortex (S1) to the early latency N1 wave is much debated. In their seminal study, Tarkka and Treede (1993) indicated that the N1 wave was generated by concomitantly active sources in both the contralateral S1 and the bilateral S2. However, most of the subsequent source analysis studies proposed dipolar modeling solutions that either did not include an S1

* Corresponding author at: Department of Neuroscience, Physiology and Pharmacology, University College London, Medical Sciences Building, Gower Street, WC1E 6BT, London, UK. Fax: +44 20 7679 7298.
E-mail address: g.iannetti@ucl.ac.uk (G.D. Iannetti).
[1] These authors contributed equally.

1053-8119/$ – see front matter © 2011 Elsevier Inc. All rights reserved.
doi:10.1016/j.neuroimage.2011.08.069

source or did not observe an improvement of the fitting when an S1 source was included in the model (Bentley et al., 2001; Bromm and Chen, 1995; Nakamura et al., 2002; Schlereth et al., 2003; Valeriani et al., 1996, 2000, 2004). This has led some authors to conclude that the parasylvian region, rather than S1, was the earliest cortical structure to respond to nociceptive input in humans (Treede et al., 2000), while others considered that the absence of S1 activation could be only apparent, and due to a combination of technical and physiological factors (e.g., Kakigi et al., 1995). Thus, it is still unclear if and how much S1 contributes to the early part of the cortical response elicited by nociceptive stimuli. This issue is an important one, as the N1 wave of the LEPs has been recently demonstrated to represent somatosensory specific activities maximally reflecting the incoming nociceptive input (Lee et al., 2009; Mouraux and Iannetti, 2009) and to present theoretical advantages for clinical application, such as its lower sensitivity to attention and vigilance as compared to the later vertex complex (Cruccu et al., 2008; Garcia-Larrea et al., 1997).

In the present study we aimed to solve this issue conclusively, by recording 64-channel LEPs elicited by the stimulation of the four limbs, in a large population of healthy volunteers ($n = 35$). In order to compensate for the limited spatial resolution of the techniques used to infer the location of the neural sources underlying scalp ERPs, we analyzed the LEP data both at group and single-subject level, using three different source analysis approaches: distributed source analysis, dipolar source modeling, and probabilistic independent component analysis (PICA).

Material and methods

Subjects

EEG data were collected from 35 healthy volunteers (18 females) aged 27 ± 4.5 (mean $\pm$ SD, range = 22 to 41 years). The present data were collected within a project aiming to investigate the placebo effect (Chakrabarti et al., 2010). All participants gave their written informed consent and were paid for their participation. The local ethics committee approved the procedures.

Nociceptive stimulation

Radiant-heat stimuli were generated by an infrared neodymium yttrium aluminum perovskite (Nd:YAP) laser with a wavelength of 1.34 μm (Electronical Engineering, Italy). Laser pulses activate directly nociceptive terminals in the most superficial skin layers (Baumgartner et al., 2005; Iannetti et al., 2006). Laser pulses were directed at the dorsum of both left and right hand and foot, on a squared area (5×5 cm) defined prior to the beginning of the experimental session. A He–Ne laser pointed to the area to be stimulated. The laser pulse was transmitted via an optic fiber and its diameter was set at approximately 6 mm (28 mm^2) by focusing lenses. The pulse duration was 4 ms. One energy of stimulation was used in each of the four conditions. The average energies were as follows: right and left hand, 2.2 ± 0.3 J; right and left foot, 2.3 ± 0.4 J. At these energies laser pulses elicited a clear pinprick pain, related to the activation of Aδ fibers. After each stimulus, the laser beam target was shifted by approximately 1 cm in a random direction, to avoid nociceptor fatigue or sensitization.

Experimental design

Before the recording session the energy of the laser stimulus was individually adjusted using the method of limits (laser step size: 0.25 J), separately for each of the four stimulated territories (left hand, right hand, left foot, right foot), to ensure that the elicited sensation was in the painful range. During this procedure subjects were asked to report the quality and the intensity of the sensation elicited by each laser pulse using a numerical rating scale (0 = no sensation, 1 = low warmth, 2 = moderate warmth, 3 = high warmth, 4 = non painful pinprick, 5 = mild pinprick pain, 6 = moderate pinprick pain, 7 = high pinprick pain, and 8 = unbearable pinprick pain). The energy of laser stimulation needed to achieve a rating of 6 was used throughout the experiment.

Laser-evoked EEG responses were obtained following the stimulation of the dorsum of the right and left hand and foot in four separate blocks, on the same day. The order of the four blocks was balanced across subjects. In each block we delivered 30 laser pulses, using an inter-stimulus interval (ISI) ranging between 5 and 15 s. At the end of each block, participants were asked to rate the intensity of the painful sensation elicited by the laser stimuli using a visual analogue scale ranging from 0 (not painful) to 100 (extremely painful).

EEG recording

Participants were seated in a comfortable chair in a silent, temperature-controlled room. They wore protective goggles and were asked to focus their attention on the stimuli and relax their muscles. The EEG was recorded using 64 Ag–AgCl scalp electrodes placed according to the International 10–20 system, referenced against the nose. Electro-oculographic (EOG) signals were simultaneously recorded using surface electrodes. Signals were amplified and digitized at a sampling rate of 1000 Hz.

EEG data pre-processing

EEG data were processed using EEGLAB (Delorme and Makeig, 2004), an open source toolbox running in the MATLAB environment. Continuous EEG data were band-pass filtered between 1 and 30 Hz. EEG epochs were extracted using a window analysis time of 1500 ms (500 ms pre-stimulus and 1000 ms post-stimulus) and baseline corrected using the pre-stimulus interval. Trials contaminated by eye-blinks and movements were corrected using an Independent Component Analysis (ICA) algorithm (Delorme and Makeig, 2004; Jung et al., 2001; Makeig et al., 1997). In all datasets, these independent components (ICs) had a large EOG channel contribution and a frontal scalp distribution. After ICA and an additional baseline correction (from −500 ms to 0 ms), EEG epochs were re-referenced to a common average reference.

In each subject, epochs belonging to the same experimental condition were averaged, time-locked to the onset of the stimulus. This procedure yielded, in each subject, four average waveforms (one waveform for each experimental condition: left hand, right hand, left foot, right foot). Single-subject average waveforms were subsequently averaged to obtain group-level average waveforms. Group-level scalp topographies were computed by spline interpolation.

Scalp topographies were first plotted at the peak latency of the N2 and P2 LEP waves, measured at the vertex (Cz) (Fig. 1). The N2 wave was defined as the most negative deflection after stimulus onset. The P2 wave was defined as the most positive deflection after stimulus onset. While N2 and P2 peaks were easily identified in all experimental conditions, N1 peaks were easily identified only in the LEP waveforms elicited by hand stimulation, using the recommended Tc–Fz montage (Kunde and Treede, 1993; Treede et al., 2003). For this reason, scalp topographies capturing the N1 activity were plotted, in steps of 10 ms, for the 60 ms time window preceding the N2 peak (hand stimulation: from 140 ms to 200 ms; foot stimulation: from 180 ms to 240 ms) (Fig. 2). This approach allowed defining better the N1 activity across time in each experimental condition.

Source analysis: group level

Group-level average LEP waveforms were imported in Brain Electrical Source Analysis software (BESA 5.3) (Scherg, 1992; Scherg and Berg, 1996). The aim of the source analysis was to (1) estimate the locations of N1 sources from the group-level average waveforms and

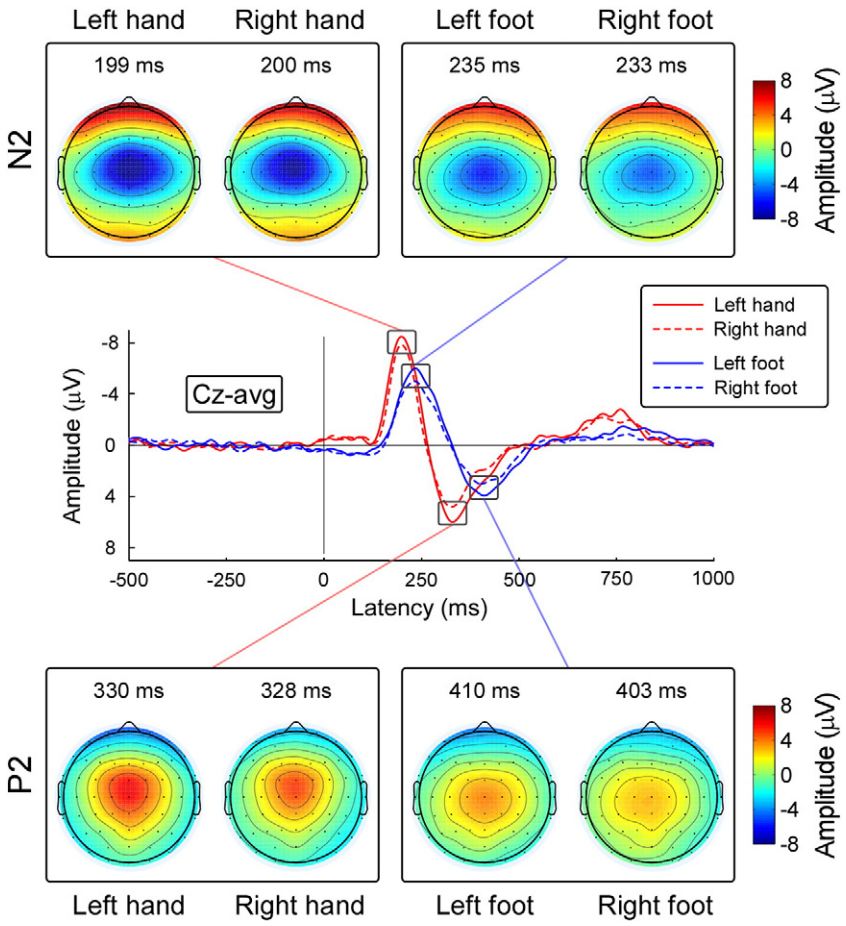

Fig. 1. N2 and P2 peaks and scalp topographies of laser-evoked potentials (LEPs). Group averages and scalp topographies of LEPs elicited by the stimulation of the hand dorsum (red waveforms) and of the foot dorsum (blue waveforms), on the left (full waveforms) and right side (dashed waveforms). Data were collected from 64 channels, in 35 subjects. Displayed signals are recorded from the vertex (Cz vs average reference). Scalp topographies are displayed at the latency of the N2 and P2 peaks, for each condition. Note that both N2 and P2 peaks are maximal at the vertex and that their scalp topographies are similar across the four stimulated territories.

(2) examine the validity of such estimated source locations. These objectives were accomplished by calculating the N1-related sources using three different approaches: (1) distributed source analysis based on Classical LORETA (Pascual-Marqui et al., 1994) Analysis Recursively Applied (CLARA; Hoechstetter et al., 2010); (2) dipole source analysis based on spatiotemporal source model (Cosandier-Rimele et al., 2006; Huizenga et al., 2002) and (3) probabilistic ICA (PICA) (Beckmann and Smith, 2004; Mouraux and Iannetti, 2009) followed by distributed source analysis using CLARA on the obtained ICs.

(1) *Distributed source analysis using CLARA.* CLARA, a newly developed iterative distributed source analysis method, was achieved by performing a weighted LORETA with a reduced source space at each iteration. As compared to LORETA (Pascual-Marqui et al., 1994), this iterative approach reduces the blurring of the estimated sources while keeping the advantage of a predefined distributed source model, thus making it easier to determine the location of the source with maximal activity (Hamalainen et al., 2011; Hoechstetter et al., 2010).
Singular value decomposition (SVD) regularization with a cutoff of 0.01% and a three iteration scheme was used to perform the CLARA source analysis (Hoechstetter et al., 2010). The locations and strengths of the regional sources were obtained for a 20-ms long interval corresponding to the earliest part of the LEP waveform elicited by hand (140–160 ms) and foot stimulation (180–200 ms). Source locations were finally transformed to Talairach space.

(2) *Discrete source analysis using dipolar modeling.* Sources of LEP waveforms were also modeled as equivalent current dipoles from a spatiotemporal source model (Huizenga et al., 2002). In this model, each dipole is specified by its location, orientation, and strength. A four-dipole model was used, according to previous reports of dipolar source analysis of LEP waveforms (Schlereth et al., 2003; Tarkka and Treede, 1993; Tsuji et al., 2006). Dipole configurations were calculated within a realistic head model and estimated according to the best correspondence between the recorded and estimated scalp distribution. Once the estimated dipoles are obtained, the corresponding model undergoes empirical evaluation of its ability to explain satisfactorily the recorded scalp topography. Such an evaluation is carried out by calculating the residual variance (RV) of the signal, i.e. the percentage of data that cannot be explained by the fitted dipoles. For each dipole, its location, orientation, and time course (i.e. its strength at every time point) were extracted. Finally, source locations were transformed to normalized Talairach space.

(3) *Distributed source analysis on independent components.* Probabilistic ICA (PICA) is an ICA (Makeig et al., 1997) constrained to an effective estimate of the intrinsic dimensionality of the original fMRI data (Beckmann and Smith, 2004). PICA has been successfully applied to the decomposition of ERP waveforms as well (Hu et al., 2011; Liang et al., 2010; Mouraux and Iannetti, 2009). When applied to multi-channel EEG recordings, ICA separates the scalp signals into a linear combination

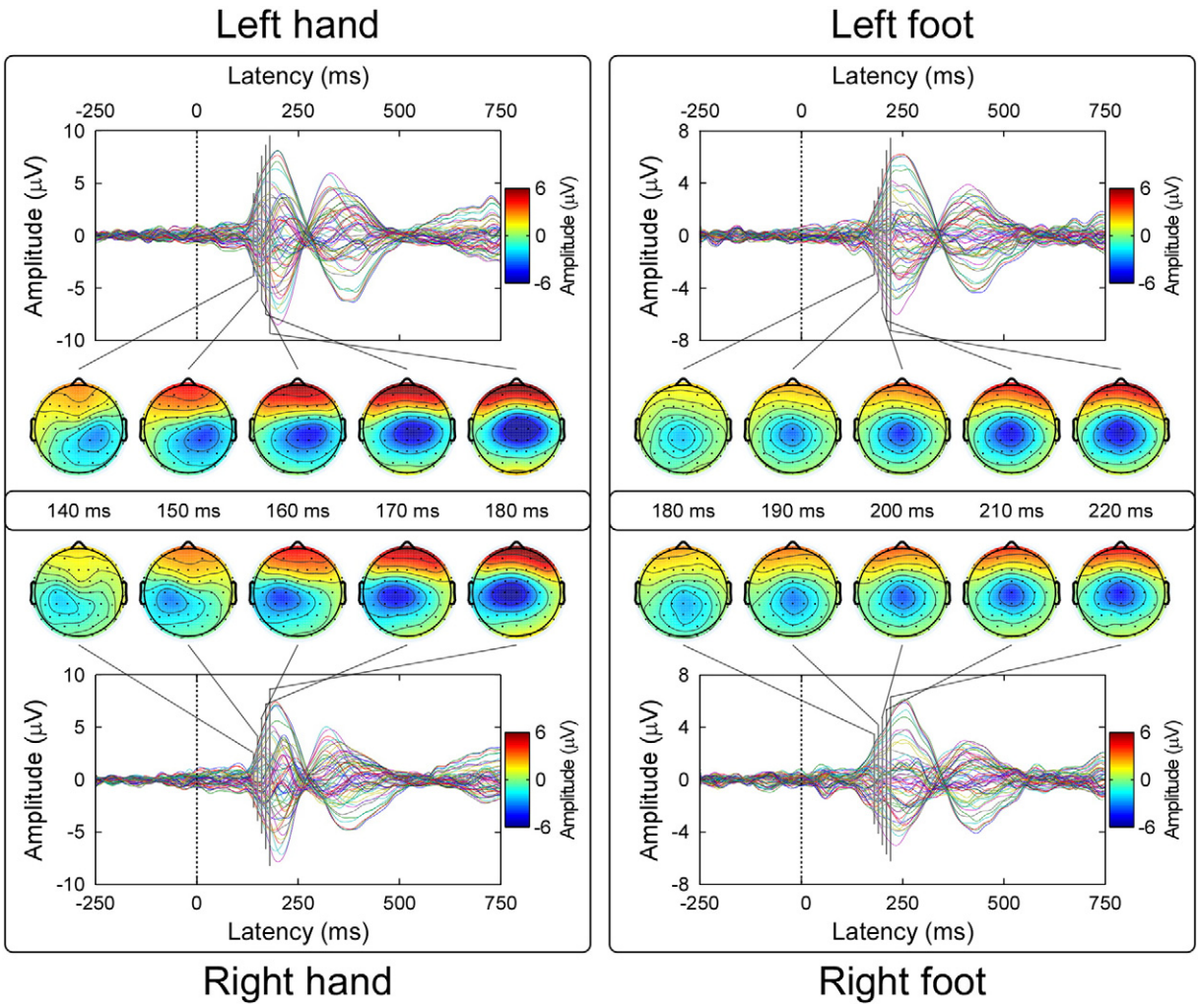

Fig. 2. Early activity and scalp topographies of laser-evoked potentials (LEPs). Group averages and scalp topographies of LEPs elicited by the stimulation of the hand dorsum (left column) and the foot dorsum (right column), on the left (upper panels) and right sides (lower panels). Data were collected from 64 channels, in 35 subjects. Signals from different electrodes are plotted in different colors and superimposed. Series of five scalp topographies of the earliest part of the LEP time course (140–180 ms for the hand LEP and 180–220 ms for the foot LEP) are displayed with a 10-ms interval. Note that the scalp topography of the early part of the response elicited by the stimulation of the hand displays a negativity contralateral to the stimulated side (left column), whereas the scalp topography of the response elicited by the stimulation of the foot is always centrally distributed. This scalp distribution is compatible with the somatotopical organization of the primary somatosensory cortex.

of ICs, each having a fixed scalp topography and a maximally independent time course. When ICA is unconstrained, the total number of estimated ICs equals the total number of recording electrodes. If the number of estimated ICs differs greatly from the actual number of independent sources contributing to the signal, this may constitute a critical problem (Beckmann and Smith, 2004). Indeed, if the number of estimated ICs is much larger than the number of sources, ICs containing spurious activity will appear because of overfitting. On the contrary, if the number of estimated ICs is much smaller than the number of sources, valuable information will be lost because of underfitting. This fundamental limitation can be addressed using PICA, a method that constrains the total number of estimated ICs to an effective estimate of the intrinsic dimensionality of the EEG data. For this reason, PICA is likely to produce a more accurate separation of intrinsic neural activities, and each IC is more likely to represent a single physiological source activity (Hu et al., 2011; Liang et al., 2010; Mouraux and Iannetti, 2009). Therefore, to verify the accuracy of the estimated generators of the N1 wave of LEPs, we performed an additional source analysis on the N1-related ICs, separated using PICA.

In each of the four stimulation conditions (left hand, right hand, left foot, and right foot), the single-subject average LEP waveforms were decomposed using PICA. Resulting ICs were classified as 'N1-related' (i.e. capturing the earliest neural activity elicited by the laser stimulus) when satisfying the following two criteria (Hu et al., 2010): (1) being stimulus-related, i.e. reflecting neural activity elicited by the laser stimulus. To ascertain this, the time course of the power of each IC (μV^2) was expressed as the standard deviation from the mean (Z scores) of the pre-stimulus interval (−500 to 0 ms). For each IC, Z scores were then averaged in the post-stimulus interval (0 to 500 ms). Only if the resulting average Z score was larger than 5, the IC was considered to reflect stimulus-evoked activity (the same approach used in Mouraux and Iannetti, 2009, and Hu et al., 2010). (2) Having a peak latency in a time window compatible with the earliest neural activities elicited by the laser stimulus (i.e. between 120 and 180 ms for hand stimulation and between 160 and 220 ms for foot stimulation).

In each of the four stimulation conditions, the scalp topography of these 'N1-related' ICs was imported into BESA (Scherg, 1992; Scherg and Berg, 1996), and the location of its sources was estimated using CLARA, as described previously. The obtained source locations were finally transformed to Talairach space.

Source analysis: individual level

Discrete source analysis using dipolar modeling

Average LEP data of each subject were also imported into BESA (Scherg, 1992; Scherg and Berg, 1996) and their sources were modeled as equivalent current dipoles from a spatiotemporal source model, using the same procedure described for group-level LEP data (Cosandier-Rimele et al., 2006; Huizenga et al., 2002). Similarly to what was performed in group-level LEP data, locations of single-subject sources were transformed to normalized Talairach space, and across-subject averages of Talairach coordinates were calculated. Both the x, y and z locations and the peak latencies of single-subject dipolar sources were compared across conditions using two-tailed paired *t* tests.

Finally, the locations of the sources estimated using the four different approaches were superimposed on the MNI brain template using MRIcroN (www.sph.sc.edu/comd/rorden/mricron).

Results

Quality and intensity of perception

All participants described the sensation elicited by the laser stimuli as clearly painful and pricking. The average ratings of the painful sensation elicited by the laser stimuli were as follows: right hand, 62.4 ± 15.4; left hand, 65.7 ± 14.2; right foot, 63.0 ± 16.8; left foot, 64.7 ± 17.5. A repeated measures, two-way analysis of variance (ANOVA) was performed on the intensity ratings with 'limb' (two levels: hand and foot) and 'side' (two levels: left and right) as main factors. Results showed no main effects of either 'limb' ($F_{1,34} = 0.006$; $P = 0.93$) or 'side' ($F_{1,34} = 2.857$; $P = 0.10$), and no interaction between the two factors ($F_{1,34} = 0.274$; $P = 0.60$).

LEP waveforms and topographies

Nd:YAP laser stimulation of all stimulated territories evoked clear and reproducible time-locked Aδ-LEPs in all subjects. Fig. 1 shows the grand average LEP waveforms at Cz with the N2 and P2 waves and the scalp maps at the corresponding peak latencies. Both the N2 and P2 had maximal amplitude at Cz. Across subjects, latencies and amplitudes of N2 and P2 peaks were as follows: N2 left hand: 215 ± 24 ms, −10.3 ± 7.1 μV; N2 right hand: 222 ± 26 ms, −8.5 ± 7.1 μV; N2 left foot: 253 ± 33 ms, −6.5 ± 4.1 μV; N2 right foot: 267 ± 46 ms, −5.8 ± 4.1 μV; P2 left hand: 337 ± 30 ms, 7.0 ± 3.7 μV; P2 right hand: 344 ± 42 ms, 6.1 ± 3.8 μV; P2 left foot: 418 ± 43 ms, 4.5 ± 2.5 μV; P2 right foot: 418 ± 51 ms, 4.2 ± 2.2 μV. Scalp maps of the N2 and P2 peaks were remarkably similar across the four stimulation conditions. As previously described (Kunde and Treede, 1993; Mouraux and Iannetti, 2008), the N2 extended bilaterally towards temporal regions, whereas the P2 was more centrally distributed.

Fig. 2 shows the grand average LEP waveforms in all channels, with the scalp distribution of the earliest cortical activity, corresponding to the latency of the N1 wave. Such 'N1 activity' encompasses the 40 ms preceding the N2 peak (hand LEP: 140–180 ms; foot LEP: 180–220 ms). The scalp topography of such early activity elicited by hand stimulation displayed a clear maximum on the central-parietal electrodes overlying the hemisphere contralateral to the stimulated side (Fig. 2, left panel). In contrast, the scalp topography of the N1 activity elicited by foot stimulation was centrally-distributed, with a maximum between Cz and Pz (Fig. 2, right panel). Thus, whereas the scalp topographies of the N1 responses elicited by the stimulation of the left and right hand were clearly different (Fig. 2, left panel), the scalp topographies of the N1 responses elicited by the stimulation of the left and right foot were not (Fig. 2, right panel).

Because of the contralateral scalp distribution of the early LEP activity elicited by hand stimulation, a bipolar montage using the contralateral temporal electrode (Tc) referenced to Fz (Tc–Fz) is recommended to detect and measure the amplitude of the N1 wave (Treede et al., 2003) (Fig. 3, left panel). However, because of the lack of a contralateral response in the scalp distribution of the early LEP activity elicited by foot stimulation, the same montage is not suitable to detect such activity as a separate wave in the LEP response (Fig. 3, right panel).

Group-level distributed source analysis

Fig. 4 shows the regional sources of the early N1 LEP activity. When the stimulus was delivered to the left hand, the N1 source was located in the hand area of the contralateral S1 (Talairach coordinates: 37, −33, 50 mm) and had a maximal intensity of 3.3 nAm/cm^3. When the stimulus was delivered to the right hand, the N1 source was also located in the hand area of the contralateral S1 (Talairach coordinates: −35, −33, 51 mm) and had a maximal intensity of 3.1 nAm/cm^3. In contrast, when the stimulus was delivered to the left and to the right foot, the N1 sources were both located in the foot area of S1 (Talairach coordinates: −3, −46, 58 mm and −3, −40, 58 mm) and had a maximal intensity of 2.7 and 2.3 nAm/cm^3, respectively.

Group-level discrete source analysis

Fig. 5 shows the time courses and locations of the estimated dipolar sources of the LEPs. Location and orientation of fitted dipoles in all four conditions are summarized in Table 1. Peak latency and strength of each dipole are summarized in Table 2. In all four conditions, the peak latencies of S1 sources were shorter than the peak latencies of the other three sources (contralateral S2, ipsilateral S2 and ACC), and the earliest part of the LEP waveform was largely explained by the S1 source. While in the LEPs elicited by hand stimulation the S1 source was localized in the hand area of the contralateral S1 (Fig. 5, top panel), in the LEPs elicited by foot stimulation the S1 source was localized in the deep hemispheric midline (foot area of SI) (Fig. 5, bottom panel). In contrast, the sources explaining the remaining parts of the LEP waveforms were remarkably similar across the four conditions. The sources explaining the time window of the N2 wave were located in the contralateral and ipsilateral S2, and in the anterior part of the cingulate cortex (ACC). Finally, the source explaining the time window of the P2 wave was located in the ACC. Note that the time course of activity of the ACC source shows two clear peaks, corresponding to the peaks of the N2 and P2 waves of the LEP waveform.

Group-level distributed source analysis on independent components

In each subject the N1-related activity was clearly captured by one IC in each of the four conditions (Fig. 6). N1-related ICs contributed to the earliest part of the LEP waveform and, across the group, accounted for 5.5 ± 1.3% of the variance of the entire LEP waveform. In LEPs elicited by left and right hand stimulation N1-related ICs showed a clear contralateral scalp distribution, with a maximum around the contralateral central electrode (Cc), and a peak latency of 160 ± 25 and 166 ± 16 ms, respectively. In LEPs elicited by left and right foot stimulation, N1-related ICs showed a central scalp distribution, with a maximum between Cz and Pz, and a peak latency of 215 ± 26 and 213 ± 23 ms, respectively.

The estimated source of N1-related ICs explaining the LEP elicited by left and right hand stimulation was located in the hand area of the contralateral somatosensory cortex (Talairach coordinates: 24, −47, 58 mm and −20, −33, 58 mm, respectively). In contrast, the estimated source of N1-related ICs explaining the LEP elicited by left and right foot stimulation was located in the foot area of the contralateral

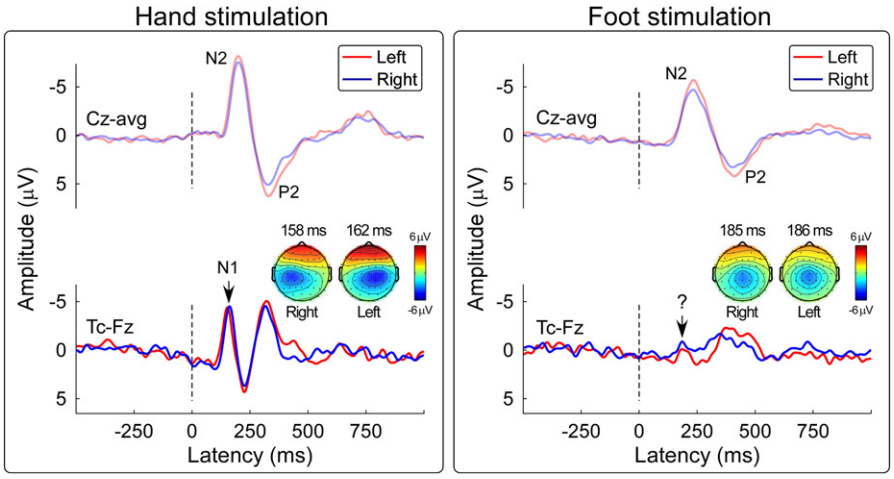

Fig. 3. Detection of the N1 wave of laser-evoked potentials (LEPs). Group averages and scalp topographies of the N1 wave of LEPs elicited by the stimulation of the hand dorsum (left panel) and the foot dorsum (right panel), on the left (red waveforms) and the right sides (blue waveforms). Data are obtained from 64 channels, in 35 subjects. The N1 wave is displayed from the contralateral temporal electrode (Tc vs Fz, as recommended in Treede et al., 2003). The N2 and P2 waves, displayed from the vertex (Cz vs average reference), are shown in pale colors for comparison. Note that, using the Tc–Fz montage, a clear N1 peak can be detected only when the stimulus is delivered on the hand dorsum, but not on the foot dorsum, as the early LEP response shows a contralateral maximum only when the hand is stimulated.

somatosensory cortex (Talairach coordinates: 4, −38, 59 mm and 4, −25, 64 mm, respectively). This finding confirms what was obtained when estimating the sources of the early part of the LEP waveforms using both distributed (regional sources) and discrete (dipoles) source analyses on raw data.

Single-subject discrete source analysis

Location and orientation of dipolar sources estimated in single-subject LEP waveforms in all four conditions are summarized in Table 1. While the locations (x, y, z) of the dipolar sources in the contralateral S2, ipsilateral S2, and ACC were not significantly different between left and right stimulation sides, for both hand and foot ($P>0.05$ in all comparisons, two-tailed paired t test), the locations of the dipolar sources in S1 were significantly different along the x axis for hand stimulation ($P<0.001$ [left hand vs right hand]) but not foot stimulation ($P>0.05$ [left foot vs right foot]). The locations of the dipolar sources in S1 were not significantly different along the y and z axes ($P>0.05$ in all comparisons, two tailed paired t test).

Peak latency and strength of these single-subject sources are summarized in Table 2. Importantly, the peak latencies of S1 sources (left hand: 154 ± 19 ms; right hand: 152 ± 19 ms; left foot: 203 ± 21 ms; right foot: 197 ± 23 ms) were significantly shorter than the peak latencies of contralateral S2 (left hand: 200 ± 34 ms; right hand: 195 ± 24 ms; left foot: 245 ± 36 ms; right foot: 239 ± 26 ms), ipsilateral S2 (left hand: 212 ± 38 ms; right hand: 208 ± 27 ms; left foot: 263 ± 42 ms; right foot: 254 ± 29 ms) and ACC (left hand: 217 ± 26 ms and 339 ± 29 ms; right hand: 216 ± 21 ms and 340 ± 32 ms; left foot: 262 ± 40 ms and 404 ± 47 ms; right foot: 260 ± 39 ms and 405 ± 48 ms) ($P<0.001$ in all comparisons, two-tailed paired t test).

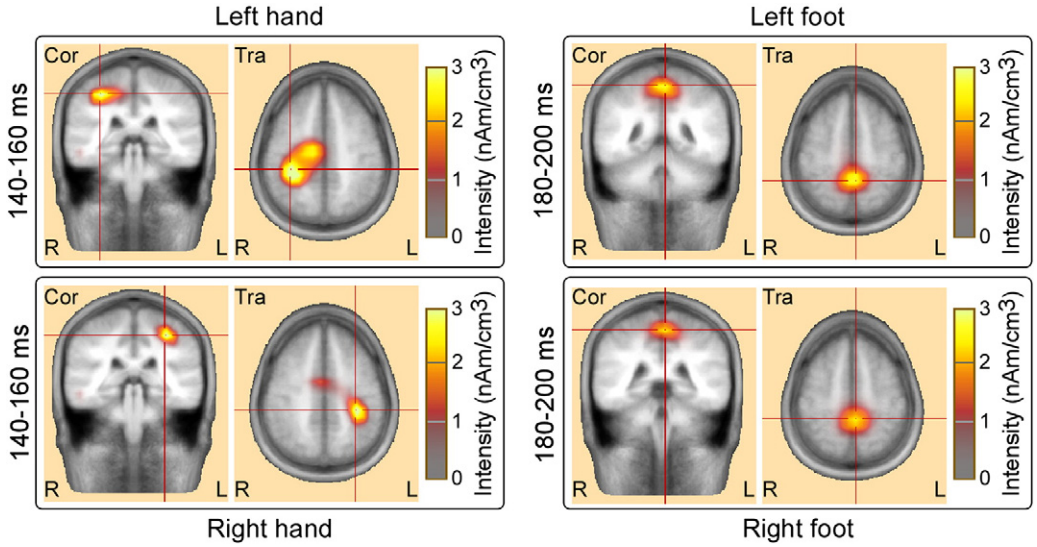

Fig. 4. Distributed source analysis of the early activity of laser-evoked potentials (LEPs). Sources of the earliest part of the group average LEP waveforms elicited by hand stimulation (140–160 ms, left column) and foot stimulation (180–200 ms, right column). Distributed sources estimated using CLARA (Hoechstetter et al., 2010) are superimposed on standard MR image template and color coded according to their intensity, expressed in nAm/cm^3. Note that the locations of the sources of the earliest part of the LEP waveform elicited by the stimulation of the hand and of the foot are only compatible with the corresponding hand and foot areas in the primary somatosensory cortex (S1).

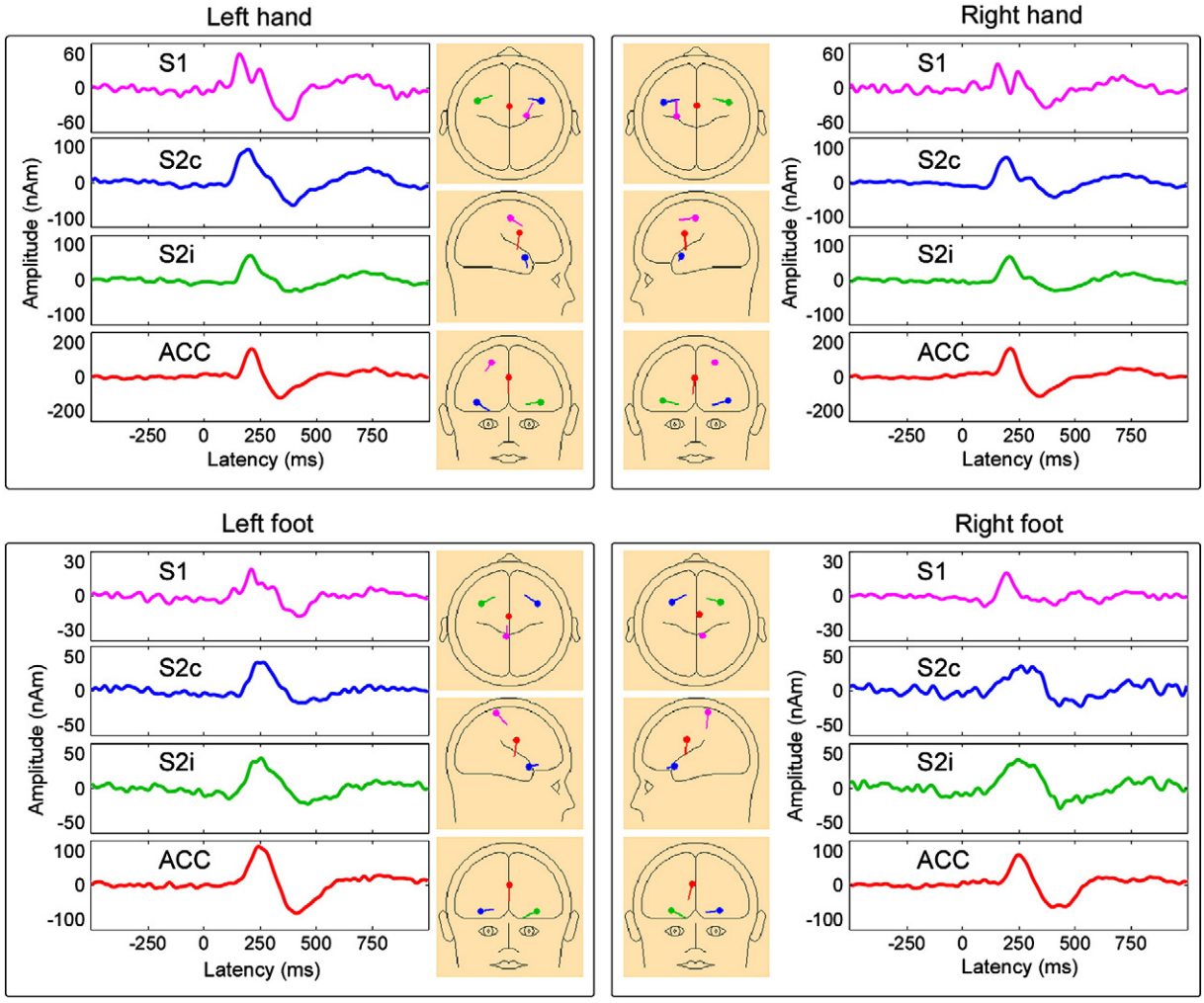

Fig. 5. Spatiotemporal dipolar source analysis of laser-evoked potentials (LEPs). Dipolar sources of the group average LEP waveforms elicited by hand stimulation (upper panel) and foot stimulation (lower panel). Dipolar sources were estimated using BESA (Cosandier-Rimele et al., 2006; Scherg and Berg, 1996), using a four-dipole model. Source locations were the primary somatosensory cortex (S1), the bilateral secondary somatosensory cortex (S2) and the anterior cingulate cortex (ACC). The time courses of dipole sources are displayed in the lateral part of each panel, and the locations and orientations of dipole sources are displayed using glass brain views in the medial part of each panel. Note that the spatial locations of contralateral S2, ipsilateral S2, and ACC dipoles are similar across the four conditions, whereas the spatial locations of the S1 dipoles vary according to the stimulated body territory (hand vs. foot). Note also that the peak in the S1 source time course displays the earliest latency (left hand: 156 ms; right hand: 157 ms; left foot: 212 ms; right foot: 201 ms) than all other time courses (Table 1).

Finally, Fig. 7 summarizes the locations of the sources explaining the earliest part of the LEP response, estimated using all the four different analyses employed: distributed source analysis on raw data, group and single-subject dipolar source analysis on raw data and distributed source analysis on the N1-related ICs.

Discussion

Our results show that the scalp distributions of the earliest part of the brain response elicited by nociceptive stimulation of the right and left hand are significantly different, as they present a clear maximum

Table 1
Latencies and strength of LEP dipolar activities.

	Stimulated district	Dipole 1 (S1)		Dipole 2 (S2c)		Dipole 3 (S2i)		Dipole 4 (ACC)			
								1st peak		2nd peak	
		Latency (ms)	Strength (nAm)	Latency (ms)	Strength (nAm)	Latency (ms)	Strength (nAm)	Latency (ms)	Strength (nAm)	Latency (ms)	Strength (nAm)
Group level	LH	156	37.2	196	75.1	205	55.5	212	127	338	−94
	RH	157	27.9	195	56.6	210	52.6	214	128	345	−87
	LF	212	25.0	239	31.9	255	33.8	244	87	413	−63
	RF	201	18.5	235	23.8	248	32.2	250	69	401	−49
Single subject level	LH (mean ± SD)	154 ± 19	46 ± 43	200 ± 34	106 ± 74	212 ± 38	82 ± 68	217 ± 26	141 ± 97	339 ± 29	−127 ± 85
	RH (mean ± SD)	152 ± 19	36 ± 27	195 ± 24	79 ± 54	208 ± 27	63 ± 44	216 ± 21	111 ± 94	340 ± 32	−117 ± 83
	LF (mean ± SD)	203 ± 21	42 ± 35	245 ± 36	71 ± 34	263 ± 42	56 ± 42	262 ± 40	77 ± 58	404 ± 47	−87 ± 49
	RF (mean ± SD)	197 ± 23	35 ± 42	239 ± 26	58 ± 51	254 ± 29	61 ± 65	260 ± 39	72 ± 61	405 ± 48	−97 ± 59

S1: primary somatosensory cortex; S2c: contralateral secondary somatosensory cortex; S2i: ipsilateral secondary somatosensory cortex; ACC: anterior cingulate cortex; LH: left hand; RH: right hand; LF: left foot; RF: right foot; ms: millisecond; nAm: nanoAmpere × meter.

Table 2
Estimated locations of the sources of the earliest part of the LEP waveform, in Talairach coordinates (mm).

	Left hand			Right hand			Left foot			Right foot		
	x	*y*	*z*	*x*	*y*	*z*	*x*	*y*	*z*	*x*	*y*	*z*
Approach 1	37	−33	50	−35	−33	51	−3	−46	58	−3	−40	58
Approach 2	23	−19	51	−25	−20	51	−4	−44	65	7	−42	66
Approach 3	24	−47	58	−20	−33	58	4	−38	59	4	−25	64
Approach 4 (mean ± SD)	23 ± 6	−16 ± 9	50 ± 11	−25 ± 5	−22 ± 15	52 ± 6	1 ± 8	−39 ± 14	60 ± 7	−5 ± 6	−41 ± 10	62 ± 6
Average	27	−29	52	−26	−27	53	−1	−42	61	1	−37	63

Approach 1: distributed source analysis (group level); Approach 2: dipolar source analysis (group level); Approach 3: distributed source analysis on early ('N1-related') ICs (group level); Approach 4: dipolar source analysis (single-subject level).

over the central-parietal electrodes *contralateral* to the stimulated side (Fig. 1). In contrast, the scalp distributions of the earliest part of the response elicited by nociceptive stimulation of the right and left foot are similar, as they present a clear maximum over the central-parietal *midline* electrodes, without any sign of lateralization (Fig. 2). These findings are compatible with the somatotopic representation of the body in the primary somatosensory cortex.

Furthermore, by using three different source analysis approaches, we provide compelling evidence that the cortical sources of the earliest part of the LEP response are located in the postcentral gyrus, in

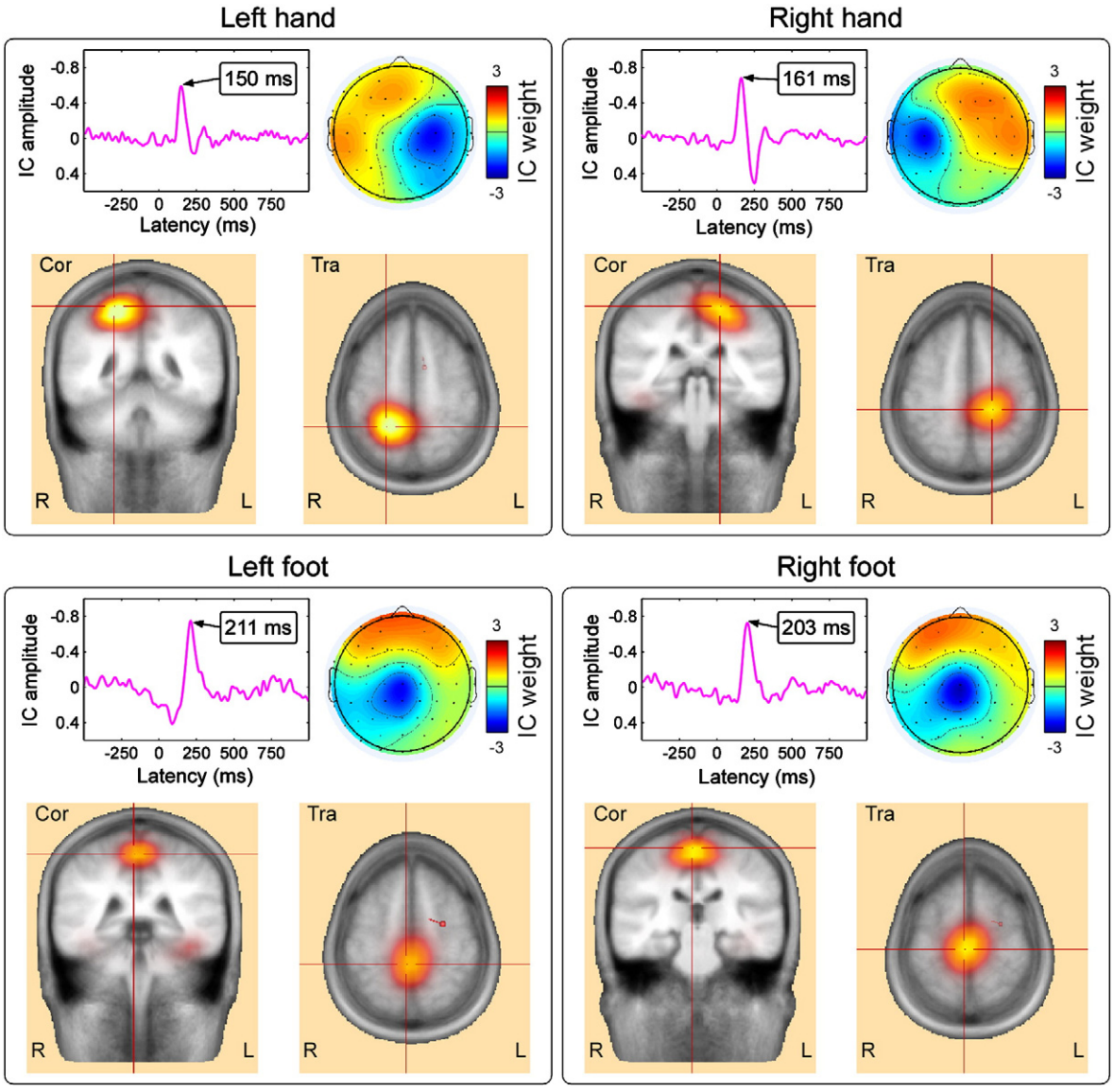

Fig. 6. ICA decomposition of laser-evoked potentials (LEPs). Waveform, topography and sources of early ('N1-related') ICs. LEP waveforms in each of the four conditions were decomposed using a probabilistic ICA approach (Beckmann and Smith, 2004). Time course, scalp topography and distributed sources of ICs reflecting the early LEP activity in each of the four conditions. All time courses show a peak with a latency corresponding to the latency of the N1 LEP peak. Note also that the scalp topography of these ICs is clearly different between the right and the left hand stimulation, with a clear maximum on the contralateral central and temporal electrodes. In contrast, the scalp distribution of N1-related ICs in both the right and left foot stimulation shows a maximum on the central-parietal electrodes (between Cz and Pz). Note that the source analysis results show a clearly contralateral source for the early 'hand' ICs (in a location compatible with the hand area of S1), and a midline source for the early 'foot' ICs (in a location compatible with the foot area of S1).

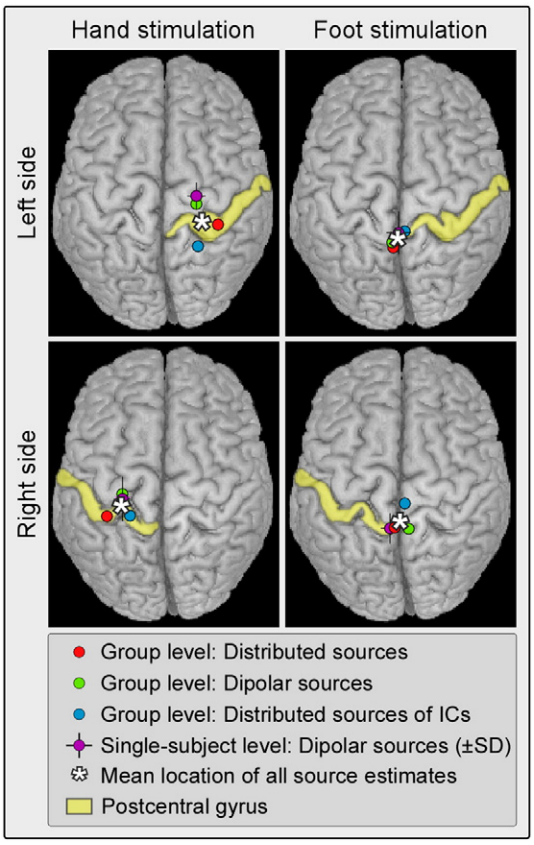

Fig. 7. Summary of all estimated locations of the sources of the earliest part of the LEP waveform. The locations of the sources of the earliest part of the LEP responses estimated both at single-subject and group level using different approaches (distributed source analysis, dipole source analysis, and distributed source analysis on the N1-related ICs). The white asterisks represent the average of the locations obtained using those approaches. The Talairach coordinates (x, y, z) of these average locations, corresponding to the hand and foot areas of the primary somatosensory cortex (S1), are as follows. Left hand stimulation (top left panel): 27, −29, 52 mm. Right hand stimulation (top right panel): −26, −27, 53 mm. Left foot stimulation (bottom left panel): −1, −42, 61 mm. Right foot stimulation (bottom right panel): 1, −37, 63 mm.

positions compatible with the corresponding representations of the stimulated body district in the primary somatosensory cortex (S1) (Figs. 4–6). Altogether, these two findings provide strong evidence that the earliest part of the scalp response elicited by a selectively nociceptive stimulus is largely explained by neural activity in S1.

Finally, both the scalp distribution and the estimated sources of the late part of the LEP response were not different across stimulated districts (Figs. 1 and 4). This finding indicates a negligible contribution of S1 to the later cortical processing elicited by transient nociceptive stimuli.

S1 responses to nociceptive stimulation

Whereas there is a general agreement that functional neuroimaging techniques (like EEG, MEG, fMRI, and positron emission tomography [PET]) reliably detect increased neural activity in S1 in response to the simulation of non-nociceptive Aβ fibers in humans, the presence of S1 responses to the stimulation of nociceptive Aδ fibers is more debated (Bushnell et al., 1999). As a matter of fact, in comparison with the constantly described responses in the thalamus, in the operculo-insular cortex, and in the cingulate cortex, responses to nociceptive stimulation in S1 are reported in approximately 75% of functional neuroimaging studies (Apkarian et al., 2005).

To ascertain whether S1 responds to nociceptive stimuli, it is crucial to employ somatosensory stimuli that activate Aδ skin nociceptors *selectively*, i.e. without the coactivation of non-nociceptive Aβ fibers. Indeed, when both populations of primary somatosensory afferents are activated (by high-intensity electrical or mechanical stimuli, for example) it is not possible to exclude that the responses in S1 are entirely explained by the tactile input concomitant to the nociceptive input. For this reason the discussion that follows considers only studies performed using nociceptive specific stimuli.

Significant S1 activations are reported in approximately 60% of the studies (published up to 2010) using PET and fMRI to record brain activity in response to *selective* nociceptive stimulation. Thus, there is robust evidence that S1 responses to Aδ input can be detected using PET and fMRI, although they cannot be conclusively distinguished in terms of intensity and spatial extent (Mouraux et al., 2011). Furthermore, fMRI and PET cannot discriminate if these Aδ-related S1 responses correspond to the early or the late phases of the cortical processing elicited by nociceptive events.

The higher ability of electrophysiological techniques like EEG and MEG to resolve neural events in time allows identifying the sequence of activation of different cortical areas (Wendel et al., 2009). However, these techniques need some prior assumptions to localize the cortical areas generating the response recorded on the scalp, and, to achieve robust results, large cohorts of subjects are needed (Babiloni et al., 2004; Whittingstall et al., 2003).

Importantly, most of the studies estimating the LEP and laser-evoked field (LEF) sources have been conducted on small populations of volunteers (commonly less than 12, e.g., Valeriani et al., 1996), and using a relatively low number of scalp channels (e.g., Tarkka and Treede, 1993; Valeriani et al., 2000). In addition to the studies using scalp EEG and MEG, a certain number of investigations employed subdural and intracranial EEG in patients to define the cortical sources of the responses evoked by nociceptive stimuli (Frot et al., 1999, 2007, 2008; Frot and Mauguiere, 2003; Kanda et al., 2000; Lenz et al., 1998a, 1998b; Ohara et al., 2004; Valeriani et al., 2004, 2009; Vogel et al., 2003). These subdural and intracranial EEG studies have the advantage of a higher spatial resolution, but at the cost of a limited spatial coverage. In addition, they record from some cortical regions more frequently than others (e.g., parasilvian more often than postcentral region), due to the clinical condition of the patient examined. Crucially, in the few patients where activity in the postcentral region was directly recorded, both the presence (Ohara et al., 2004) and the absence (Valeriani et al., 2004) of responses to laser nociceptive stimuli have been reported.

In the present study we collected data from one of the largest sample of subjects ever used in a single experiment employing selective nociceptive stimuli. This resulted in improved accuracy of the topographical LEP maps (Figs. 1 and 2) and of the estimated neural sources (Figs. 4, 5 and 6). The S1 source explained virtually the entirety of the earliest 20 ms of the cortical response elicited by laser stimuli (i.e. 140–160 ms for the LEP elicited by hand stimulation and 180–200 ms for the LEP elicited by foot stimulation) (Figs. 4–6). This finding was obtained using different source analysis approaches, based on very different assumptions, either hypothesis-driven (equivalent current dipoles; Fig. 5) or data-driven (distributed sources [CLARA] and spatial independency of source responses [PICA + CLARA]; Figs. 4 and 6). The combination of such different approaches minimizes the intrinsically limited trustworthiness of each of them, giving confidence that the estimated sources reflect the actual neural generators of the recorded LEPs (Fig. 7). Notably, many of the studies that failed to detect S1 activity relied solely on the hypothesis-driven, equivalent dipolar modeling approach (e.g. Bromm and Chen, 1995; Valeriani et al., 1996, 2000).

Early cortical responses to nociceptive stimulation: S1 vs S2

Accumulating and convincing experimental evidence, obtained by scalp, epidural and intracranial EEG recordings, has led to the general agreement that the operculoinsular region (i.e. S2 and the posterior area of the insular cortex) generates early responses to incoming

nociceptive input (Frot et al., 2007, 2008; Frot and Mauguiere, 2003; Kakigi et al., 1995; Kanda et al., 2000; Perchet et al., 2008; Valeriani et al., 1996, 2000; Vogel et al., 2003). In contrast, as discussed above, whether S1 contributes to the early part of the LEP response has been largely debated since the pioneer study of Tarkka and Treede (1993). Our results indicate not only that S1 responds at the earliest stages of the LEP response (Figs. 2 and 3), but also that such S1 response contributes almost entirely to the earliest LEP response (in a time window corresponding to the latency of the N1 wave elicited by hand stimulation: 140–160 ms). These findings have important implications, as most experimental results in the LEP literature, including those from our own group, have been discussed considering the N1 wave as being largely generated in S2, with, possibly, some contribution from S1 (e.g. Garcia-Larrea et al. 2003; Iannetti et al., 2005; Valeriani et al., 2008; Valentini et al., 2011). Our results do not exclude a contribution of S2 and insular cortex to the early LEP response, but undoubtedly indicate that a possible S2/insular contribution to its earliest part (i.e. up to 160 ms following hand stimulation and up to 200 ms following foot stimulation) is, if any, minimal.

The robust evidence that S2 shows early responses to nociceptive input (Frot et al., 2001; Frot and Mauguiere, 2003) is not in contradiction with what we observed. Indeed, the main response recorded invasively in S2 peaks at 170 ms (see, for example, Fig. 1 of Frot et al., 2001, and Fig. 1 of Frot and Mauguiere, 2003), i.e. a latency at which the scalp lateralization effect we observed has already vanished, and the S1 source (140–160 ms) has already finished to contribute to the LEP waveform (Figs. 1–3). Whether the early responses we observed in S1 and those recorded invasively in S2 are consequent to a thalamus-to-S1 input that is then relayed from S1 to S2/insula in a serial fashion (Allison et al., 1989; Hari et al., 1993), or to a parallel processing from the thalamus (Ploner et al., 1999; Pons et al., 1992) remains an open question. Recent evidence from functional connectivity analysis of fMRI data using Dynamic Causal Modeling (DCM) indicates that both tactile and nociceptive inputs are, at least partly, processed serially from S1 to S2 (Liang et al., 2011). The present results might provide the temporal dimension of this effect, suggesting that the S1 activity represents the first arrival of the thalamo-cortical input, which is, in turn, relayed to the operculoinsular area.

The N1 wave: practical implications in LEP studies

In recent years, there has been a growing interest in understanding the experimental modulations of the latency and amplitude of the N1 LEP wave, and to characterize its functional significance (Ellrich et al., 2007; Iannetti et al., 2008; Lee et al., 2009; Legrain et al., 2002; Mouraux and Iannetti, 2009; Schmahl et al., 2004). As the N1 wave represents an early stage of sensory processing more directly related to the ascending nociceptive input (Lee et al., 2009), a more systematical examination of N1 has been recommended to enhance the sensitivity of LEPs in clinical applications (Cruccu et al., 2008; Treede et al., 2003), and methods to enhance its signal-to-noise ratio and estimate automatically its latency and amplitude have been developed (Hu et al., 2010).

Our result that the largest part of the neural activity underlying the N1 wave time window arises from S1 (Fig. 3) has practical implications in the detection of this LEP wave. Indeed, to optimally detect and measure the N1 wave, a montage using the temporal or the central electrode contralateral to the stimulated hand (Tc or Cc) referenced to Fz is commonly recommended (Cruccu et al., 2008; Hu et al., 2010), as its scalp topography displays a positive maximum contralateral to the stimulated side (Kunde and Treede, 1993; Tarkka and Treede, 1993). Crucially, these studies used hand stimulation to elicit the LEPs. Our data show that such recommended montage is optimal only when examining the LEP elicited by hand stimulation, but it does not allow detecting an N1 wave when the LEP is elicited by foot stimulation (Fig. 3). This observation, consequent to the midline location of the foot area in the S1 somatotopical map (Jasper and Penfield, 1954), clearly indicates that the EEG montages to isolate and measure the earliest activity in the LEP waveform should be defined as a function of the somatotopical representation of the stimulated body district in S1. Indeed, the Tc–Fz or Cc–Fz montages would be optimal for identifying the N1 wave elicited by hand stimulation, while more lateral and anterior electrodes (e.g. C5–Fz, Fc5–Fz and C6–Fz, Fc6–Fz) along the postcentral sulcus are probably more suitable to identify the N1 wave elicited by trigeminal stimulation (Cruccu et al., 1999). Importantly, the early cortical activity evoked by laser stimulation of the foot is not appropriately captured with the Tc–Fz montage. Because of its midline generators, such cortical activity is difficult to be isolated as a separate deflection on the LEP waveform.

Acknowledgments

E. Valentini is supported by The British Academy (small research grant scheme). G.D. Iannetti is a University Research Fellow of The Royal Society and acknowledges the support of the BBSRC. Data collection on this project was partly supported by a British Council Researcher Exchange grant to B. Chakrabarti. All authors are grateful to the members of the GAMFI Project (part of the IannettiLab: http://iannettilab.webnode.com) for insightful comments. The authors acknowledge the generous support of El.En.

References

Allison, T., McCarthy, G., Wood, C.C., Darcey, T.M., Spencer, D.D., Williamson, P.D., 1989. Human cortical potentials evoked by stimulation of the median nerve I. Cytoarchitectonic areas generating short-latency activity. J. Neurophysiol. 62, 694–710.

Apkarian, A.V., Bushnell, M.C., Treede, R.D., Zubieta, J.K., 2005. Human brain mechanisms of pain perception and regulation in health and disease. Eur. J. Pain 9, 463–484.

Babiloni, F., Babiloni, C., Carducci, F., Romani, G.L., Rossini, P.M., Angelone, L.M., Cincotti, F., 2004. Multimodal integration of EEG and MEG data: a simulation study with variable signal-to-noise ratio and number of sensors. Hum. Brain Mapp. 22, 52–62.

Baumgartner, U., Cruccu, G., Iannetti, G.D., Treede, R.D., 2005. Laser guns and hot plates. Pain 116, 1–3.

Beckmann, C.F., Smith, S.M., 2004. Probabilistic independent component analysis for functional magnetic resonance imaging. IEEE Trans. Med. Imaging 23, 137–152.

Bentley, D.E., Youell, P.D., Crossman, A.R., Jones, A.K., 2001. Source localisation of 62-electrode human laser pain evoked potential data using a realistic head model. Int. J. Psychophysiol. 41, 187–193.

Bromm, B., Chen, A.C., 1995. Brain electrical source analysis of laser evoked potentials in response to painful trigeminal nerve stimulation. Electroencephalogr. Clin. Neurophysiol. 95, 14–26.

Bromm, B., Treede, R.D., 1984. Nerve fibre discharges, cerebral potentials and sensations induced by CO_2 laser stimulation. Hum. Neurobiol. 3, 33–40.

Bushnell, M.C., Duncan, G.H., Hofbauer, R.K., Ha, B., Chen, J.I., Carrier, B., 1999. Pain perception: is there a role for primary somatosensory cortex? Proc. Natl. Acad. Sci. U. S. A. 96, 7705–7709.

Carmon, A., Mor, J., Goldberg, J., 1976. Evoked cerebral responses to noxious thermal stimuli in humans. Exp. Brain Res. 25, 103–107.

Chakrabarti, B., Valentini, E., Aglioti, S.M., 2010. Empathy Modulates the Neural Correlates of Placebo Analgesia: A Laser Evoked Potential (LEP) Study. Society for Neuroscience, San Diego, CA.

Cosandier-Rimele, D., Badier, J.M., Wendling, F., 2006. A realistic spatiotemporal source model for EEG activity: application to the reconstruction of epileptic depth-EEG signals. Conf. Proc. IEEE Eng. Med. Biol. Soc. 1, 4253–4256.

Cruccu, G., Romaniello, A., Amantini, A., Lombardi, M., Innocenti, P., Manfredi, M., 1999. Assessment of trigeminal small-fiber function: brain and reflex responses evoked by CO_2-laser stimulation. Muscle Nerve 22, 508–516.

Cruccu, G., Aminoff, M.J., Curio, G., Guerit, J.M., Kakigi, R., Mauguiere, F., Rossini, P.M., Treede, R.D., Garcia-Larrea, L., 2008. Recommendations for the clinical use of somatosensory-evoked potentials. Clin. Neurophysiol. 119, 1705–1719.

Delorme, A., Makeig, S., 2004. EEGLAB: an open source toolbox for analysis of single-trial EEG dynamics including independent component analysis. J. Neurosci. Methods 134, 9–21.

Ellrich, J., Jung, K., Ristic, D., Yekta, S.S., 2007. Laser-evoked cortical potentials in cluster headache. Cephalalgia 27, 510–518.

Frot, M., Mauguiere, F., 2003. Dual representation of pain in the operculo-insular cortex in humans. Brain 126, 438–450.

Frot, M., Rambaud, L., Guenot, M., Mauguiere, F., 1999. Intracortical recordings of early pain-related CO_2-laser evoked potentials in the human second somatosensory (SII) area. Clin. Neurophysiol. 110, 133–145.

Frot, M., Garcia-Larrea, L., Guenot, M., Mauguiere, F., 2001. Responses of the supra-sylvian (SII) cortex in humans to painful and innocuous stimuli. A study using intra-cerebral recordings. Pain 94, 65–73.

Frot, M., Magnin, M., Mauguiere, F., Garcia-Larrea, L., 2007. Human SII and posterior insula differently encode thermal laser stimuli. Cereb. Cortex 17, 610–620.
Frot, M., Mauguiere, F., Magnin, M., Garcia-Larrea, L., 2008. Parallel processing of nociceptive A-delta inputs in SII and midcingulate cortex in humans. J. Neurosci. 28, 944–952.
Garcia-Larrea, L., Peyron, R., Laurent, B., Mauguiere, F., 1997. Association and dissociation between laser-evoked potentials and pain perception. Neuroreport 8, 3785–3789.
Garcia-Larrea, L., Frot, M., Valeriani, M., 2003. Brain generators of laser-evoked potentials: from dipoles to functional significance. Neurophysiol. Clin. 33, 279–292.
Haanpaa, M., Attal, N., Backonja, M., Baron, R., Bennett, M., Bouhassira, D., Cruccu, G., Hansson, P., Haythornthwaite, J.A., Iannetti, G.D., Jensen, T.S., Kauppila, T., Nurmikko, T.J., Rice, A.S., Rowbotham, M., Serra, J., Sommer, C., Smith, B.H., Treede, R.D., 2011. NeuPSIG guidelines on neuropathic pain assessment. Pain 152, 14–27.
Hamalainen, J.A., Ortiz-Mantilla, S., Benasich, A.A., 2011. Source localization of event-related potentials to pitch change mapped onto age-appropriate MRIs at 6 months of age. NeuroImage 54, 1910–1918.
Hari, R., Karhu, J., Hamalainen, M., Knuutila, J., Salonen, O., Sams, M., Vilkman, V., 1993. Functional organization of the human first and second somatosensory cortices: a neuromagnetic study. Eur. J. Neurosci. 5, 724–734.
Hoechstetter, K., Berg, P., Scherg, M., 2010. BESA Research Tutorial 4: Distributed Source Imaging.
Hu, L., Mouraux, A., Hu, Y., Iannetti, G.D., 2010. A novel approach for enhancing the signal-to-noise ratio and detecting automatically event-related potentials (ERPs) in single trials. NeuroImage 50, 99–111.
Hu, L., Zhang, Z.G., Hung, Y.S., Luk, K.D., Iannetti, G.D., Hu, Y., 2011. Single-trial detection of somatosensory evoked potentials by probabilistic independent component analysis and wavelet filtering. Clin. Neurophysiol. 122 (7), 1429–1439.
Huizenga, H.M., de Munck, J.C., Waldorp, L.J., Grasman, R.P., 2002. Spatiotemporal EEG/MEG source analysis based on a parametric noise covariance model. IEEE Trans. Biomed. Eng. 49, 533–539.
Iannetti, G.D., Truini, A., Romaniello, A., Galeotti, F., Rizzo, C., Manfredi, M., Cruccu, G., 2003. Evidence of a specific spinal pathway for the sense of warmth in humans. J. Neurophysiol. 89, 562–570.
Iannetti, G.D., Zambreanu, L., Cruccu, G., Tracey, I., 2005. Operculoinsular cortex encodes pain intensity at the earliest stages of cortical processing as indicated by amplitude of laser-evoked potentials in humans. Neuroscience 131, 199–208.
Iannetti, G.D., Zambreanu, L., Tracey, I., 2006. Similar nociceptive afferents mediate psychophysical and electrophysiological responses to heat stimulation of glabrous and hairy skin in humans. J. Physiol. 577, 235–248.
Iannetti, G.D., Hughes, N.P., Lee, M.C., Mouraux, A., 2008. Determinants of laser-evoked EEG responses: pain perception or stimulus saliency? J. Neurophysiol. 100, 815–828.
Jasper, H., Penfield, W., 1954. Epilepsy and the Functional Anatomy of the Human Brain, 2nd edition. Little, Brown and Co, Boston.
Jung, T.P., Makeig, S., Westerfield, M., Townsend, J., Courchesne, E., Sejnowski, T.J., 2001. Analysis and visualization of single-trial event-related potentials. Hum. Brain Mapp. 14, 166–185.
Kakigi, R., Koyama, S., Hoshiyama, M., Kitamura, Y., Shimojo, M., Watanabe, S., 1995. Pain-related magnetic fields following painful CO_2 laser stimulation in man. Neurosci. Lett. 192, 45–48.
Kanda, M., Nagamine, T., Ikeda, A., Ohara, S., Kunieda, T., Fujiwara, N., Yazawa, S., Sawamoto, N., Matsumoto, R., Taki, W., Shibasaki, H., 2000. Primary somatosensory cortex is actively involved in pain processing in human. Brain Res. 853, 282–289.
Kunde, V., Treede, R.D., 1993. Topography of middle-latency somatosensory evoked potentials following painful laser stimuli and non-painful electrical stimuli. Electroencephalogr. Clin. Neurophysiol. 88, 280–289.
Lee, M.C., Mouraux, A., Iannetti, G.D., 2009. Characterizing the cortical activity through which pain emerges from nociception. J. Neurosci. 29, 7909–7916.
Legrain, V., Guerit, J.M., Bruyer, R., Plaghki, L., 2002. Attentional modulation of the nociceptive processing into the human brain: selective spatial attention, probability of stimulus occurrence, and target detection effects on laser evoked potentials. Pain 99, 21–39.
Lenz, F.A., Rios, M., Chau, D., Krauss, G.L., Zirh, T.A., Lesser, R.P., 1998a. Painful stimuli evoke potentials recorded from the parasylvian cortex in humans. J. Neurophysiol. 80, 2077–2088.
Lenz, F.A., Rios, M., Zirh, A., Chau, D., Krauss, G., Lesser, R.P., 1998b. Painful stimuli evoke potentials recorded over the human anterior cingulate gyrus. J. Neurophysiol. 79, 2231–2234.
Liang, M., Mouraux, A., Chan, V., Blakemore, C., Iannetti, G.D., 2010. Functional characterisation of sensory ERPs using probabilistic ICA: effect of stimulus modality and stimulus location. Clin. Neurophysiol. 121, 577–587.
Liang, M., Mouraux, A., Iannetti, G.D., 2011. Parallel processing of nociceptive and non-nociceptive somatosensory information in the human primary and secondary somatosensory cortices: evidence from dynamic causal modeling of functional magnetic resonance imaging data. J. Neurosci. 31, 8976–8985.
Makeig, S., Jung, T.P., Bell, A.J., Ghahremani, D., Sejnowski, T.J., 1997. Blind separation of auditory event-related brain responses into independent components. Proc. Natl. Acad. Sci. U. S. A. 94, 10979–10984.
Mouraux, A., Iannetti, G.D., 2008. Across-trial averaging of event-related EEG responses and beyond. Magn. Reson. Imaging 26, 1041–1054.
Mouraux, A., Iannetti, G.D., 2009. Nociceptive laser-evoked brain potentials do not reflect nociceptive-specific neural activity. J. Neurophysiol. 101, 3258–3269.
Mouraux, A., Guerit, J.M., Plaghki, L., 2003. Non-phase locked electroencephalogram (EEG) responses to CO_2 laser skin stimulations may reflect central interactions between A partial partial differential- and C-fibre afferent volleys. Clin. Neurophysiol. 114, 710–722.
Mouraux, A., Diukova, A., Lee, M.C., Wise, R.G., Iannetti, G.D., 2011. A multisensory investigation of the functional significance of the "pain matrix". NeuroImage 54, 2237–2249.
Nakamura, Y., Paur, R., Zimmermann, R., Bromm, B., 2002. Attentional modulation of human pain processing in the secondary somatosensory cortex: a magnetoencephalographic study. Neurosci. Lett. 328, 29–32.
Ohara, S., Crone, N.E., Weiss, N., Treede, R.D., Lenz, F.A., 2004. Cutaneous painful laser stimuli evoke responses recorded directly from primary somatosensory cortex in awake humans. J. Neurophysiol. 91, 2734–2746.
Pascual-Marqui, R.D., Michel, C.M., Lehmann, D., 1994. Low resolution electromagnetic tomography: a new method for localizing electrical activity in the brain. Int. J. Psychophysiol. 18, 49–65.
Perchet, C., Godinho, F., Mazza, S., Frot, M., Legrain, V., Magnin, M., Garcia-Larrea, L., 2008. Evoked potentials to nociceptive stimuli delivered by CO_2 or Nd:YAP lasers. Clin. Neurophysiol. 119, 2615–2622.
Ploner, M., Schmitz, F., Freund, H.J., Schnitzler, A., 1999. Parallel activation of primary and secondary somatosensory cortices in human pain processing. J. Neurophysiol. 81, 3100–3104.
Pons, T.P., Garraghty, P.E., Mishkin, M., 1992. Serial and parallel processing of tactual information in somatosensory cortex of rhesus monkeys. J. Neurophysiol. 68, 518–527.
Scherg, M., 1992. Functional imaging and localization of electromagnetic brain activity. Brain Topogr. 5, 103–111.
Scherg, M., Berg, P., 1996. New concepts of brain source imaging and localization. Electroencephalogr. Clin. Neurophysiol. Suppl. 46, 127–137.
Schlereth, T., Baumgartner, U., Magerl, W., Stoeter, P., Treede, R.D., 2003. Left-hemisphere dominance in early nociceptive processing in the human parasylvian cortex. NeuroImage 20, 441–454.
Schmahl, C., Greffrath, W., Baumgartner, U., Schlereth, T., Magerl, W., Philipsen, A., Lieb, K., Bohus, M., Treede, R.D., 2004. Differential nociceptive deficits in patients with borderline personality disorder and self-injurious behavior: laser-evoked potentials, spatial discrimination of noxious stimuli, and pain ratings. Pain 110, 470–479.
Tarkka, I.M., Treede, R.D., 1993. Equivalent electrical source analysis of pain-related somatosensory evoked potentials elicited by a CO_2 laser. J. Clin. Neurophysiol. 10, 513–519.
Treede, R.D., 1995. Peripheral acute pain mechanisms. Ann. Med. 27 (2), 213–216.
Treede, R.D., 2003. Neurophysiological studies of pain pathways in peripheral and central nervous system disorders. J. Neurol. 250 (10), 1152–1161.
Treede, R.D., Apkarian, A.V., Bromm, B., Greenspan, J.D., Lenz, F.A., 2000. Cortical representation of pain: functional characterization of nociceptive areas near the lateral sulcus. Pain 87, 113–119.
Treede, R.D., Lorenz, J., Baumgartner, U., 2003. Clinical usefulness of laser-evoked potentials. Neurophysiol. Clin. 33, 303–314.
Tsuji, T., Inui, K., Kojima, S., Kakigi, R., 2006. Multiple pathways for noxious information in the human spinal cord. Pain 123, 322–331.
Valentini, E., Torta, D.M., Mouraux, A., Iannetti, G.D., 2011. Dishabituation of laser-evoked EEG responses: dissecting the effect of certain and uncertain changes in stimulus modality. J. Cogn. Neurosci. 23 (10), 2822–2837.
Valeriani, M., Rambaud, L., Mauguiere, F., 1996. Scalp topography and dipolar source modelling of potentials evoked by CO_2 laser stimulation of the hand. Electroencephalogr. Clin. Neurophysiol. 100, 343–353.
Valeriani, M., Restuccia, D., Barba, C., Le Pera, D., Tonali, P., Mauguiere, F., 2000. Sources of cortical responses to painful CO(2) laser skin stimulation of the hand and foot in the human brain. Clin. Neurophysiol. 111, 1103–1112.
Valeriani, M., Barba, C., Le Pera, D., Restuccia, D., Colicchio, G., Tonali, P., Gagliardo, O., Treede, R.D., 2004. Different neuronal contribution to N20 somatosensory evoked potential and to CO_2 laser evoked potentials: an intracerebral recording study. Clin. Neurophysiol. 115, 211–216.
Valeriani, M., Betti, V., Le Pera, D., De Armas, L., Miliucci, R., Restuccia, D., Avenanti, A., Aglioti, S.M., 2008. Seeing the pain of others while being in pain: a laser-evoked potentials study. NeuroImage 40, 1419–1428.
Valeriani, M., Truini, A., Le Pera, D., Insola, A., Galeotti, F., Petrachi, C., Mazzone, P., Cruccu, G., 2009. Laser evoked potential recording from intracerebral deep electrodes. Clin. Neurophysiol. 120, 790–795.
Vogel, H., Port, J.D., Lenz, F.A., Solaiyappan, M., Krauss, G., Treede, R.D., 2003. Dipole source analysis of laser-evoked subdural potentials recorded from parasylvian cortex in humans. J. Neurophysiol. 89, 3051–3060.
Wendel, K., Vaisanen, O., Malmivuo, J., Gencer, N.G., Vanrumste, B., Durka, P., Magjarevic, R., Supek, S., Pascu, M.L., Fontenelle, H., Grave de Peralta Menendez, R., 2009. EEG/MEG source imaging: methods, challenges, and open issues. Comput. Intell. Neurosci. 656092.
Whittingstall, K., Stroink, G., Gates, L., Connolly, J.F., Finley, A., 2003. Effects of dipole position, orientation and noise on the accuracy of EEG source localization. Biomed. Eng. Online 2, 14.